Elsevier Editorial System(tm) for Composites Part A

Manuscript Draft

Manuscript Number:

Title: Formulation and implementation of decohesion elements in an explicit finite element code

Article Type: Research Paper

Section/Category:

Keywords:

Corresponding Author: Mr Silvestre Taveira Pinho,

Corresponding Author's Institution: Imperial College London

First Author: Silvestre Taveira Pinho

Order of Authors: Silvestre Taveira Pinho; Lorenzo Iannucci, PhD; Paul Robinson, PhD

Manuscript Region of Origin:

Abstract: A decohesion element, with three different optional constitutive laws, has been implemented in an explicit finite element code. The formulation is fully three-dimensional, and can simulate mixed-mode delamination. The first constitutive law is bilinear, the second is a third-order polynomial and the third is a combination of linear and polynomial segments. The bilinear law is found to be less stable than the others under certain numerical conditions. Application examples, including mixed-mode fracture, are presented for all constitutive laws.

Formulation and implementation of decohesion elements in an explicit finite element code

S T Pinho [a], L Iannucci [a], P Robinson [a]

[a] *Department of Aeronautics, South Kensington Campus, Imperial College London, SW7 2AZ, London, U.K.*

Abstract

A decohesion element, with three different optional constitutive laws, has been implemented in an explicit finite element code. The formulation is fully three-dimensional, and can simulate mixed-mode delamination. The first constitutive law is bilinear, the second is a third-order polynomial and the third is a combination of linear and polynomial segments. The bilinear law is found to be less stable than the others under certain numerical conditions. Application examples, including mixed-mode fracture, are presented for all constitutive laws.

Key words: B Delamination, C Finite Element Analysis (FEA), Decohesion Element

Email addresses: silvestre.pinho@imperial.ac.uk (S T Pinho), l.iannucci@imperial.ac.uk (L Iannucci), p.robinson@imperial.ac.uk (P Robinson).

1 Introduction

Initiation and propagation of delamination is often a precursor to ultimate failure in laminated composite structures. Knowledge of delamination and ability to model this aspect of failure therefore deserve particular attention.

In implicit Finite Element (FE) FE codes, decohesion elements have been successfully used to simulate of standard delamination toughness tests (Double Cantilever Beam (DCB), Mixed-Mode Bending (MMB) and End Notch Flexure (ENF)) [1–6]; debonding of skin/stiffener specimens [2], overlap tests [7], compression after impact (CAI) of composite plates [1,8] and crush of composite tubes [9]. In explicit analyses, some work using a cohesive zone approach is presented in Refs. [10,11], in which the applications include MMB specimens and the impact with penetration of a steel ball in a composite plate.

LS-Dyna [12] is one of the explicit FE codes most widely used by the industry to model impact or crash situations in laminated composite materials. However, decohesion elements are not available within the code. In this work, a decohesion element with a bilinear constitutive law is formulated and implemented in LS-Dyna. The formulation is based on published work [1,6,9]. Due to stability limitations which are identified with the discontinuities in the bilinear law, two other constitutive laws are also developed. One of these constitutive laws is a third-order polynomial, and the other is a combination of linear and third-order polynomial segments. These two constitutive laws are implemented together with the bilinear law within a new decohesion element, using an enhanced formalism. The three different constitutive laws are compared, and applications are presented in mode I, II and mixed mode.

2 Bilinear constitutive law

2.1 Introduction

The bilinear formulation presented in this section is based on the formulation from Refs. [1,6,9], and a comparison with the work from Refs. [7,8,13] is performed.

Consider a point in an interface like the one in Fig. 1. The tractions t_i between the top and bottom surfaces of the interface at that point are related to the relative displacement δ_i at the same point for $i = 1, 2, 3$ (Fig. 1). The index value $i = 1$ corresponds to an opening mode (mode I), while the index values $i = 2$ and 3 correspond to a shear mode (mode II, III, or a combination of both). In decohesion-element formulations, the sliding mode is usually considered to represent both modes II and III because the distinction between mode II and III depends on the direction of the relative displacement between homologous points with respect to the orientation of the crack front. Without knowing how the crack front is oriented—and in a generic situation, with multiple crack growth, it might be difficult even to define it—it is impossible to distinguish between mode II and mode III.

The relative-displacements and tractions corresponding to the onset of damage are denoted as onset displacements and onset tractions respectively, and identified with the superscript '^{o}'. The relative displacements corresponding to complete decohesion are denoted final displacements and identified with the superscript '^{f}'.

Suppose a point loaded such that a relative displacement δ_i is applied parallel

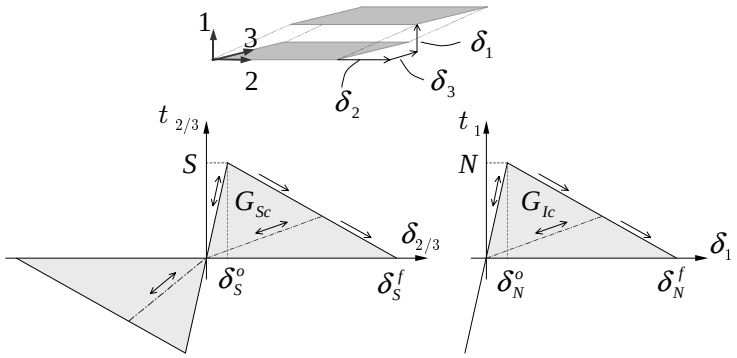

Fig. 1. Bilinear constitutive law in single-mode loading

to one of the local axes ($i = 1, 2$ or 3). While the relative displacement has never exceeded its damage onset value, the point behaves elastically. Once the onset displacement is exceeded, some energy is absorbed. The total energy that can be absorbed at each point (per unit area of the interface) equals the critical energy release rate for the corresponding mode.

When the maximum traction N or S (according to the mode) is reached, the damage is assumed to start propagating. The corresponding onset displacements are, for the opening and shear modes respectively:

$$\delta_N^o = \frac{N}{k},\ \delta_S^o = \frac{S}{k}. \tag{1}$$

When the traction reaches zero, the energy absorbed must equal the critical energy release rate. This leads directly to the definition of the final displacements in a pure-mode loading situation as

$$\delta_N^f = \frac{2G_{Ic}}{k\delta_N^o} \qquad \text{and} \qquad \delta_S^f = \frac{2G_{Sc}}{k\delta_S^o}. \tag{2}$$

2.2 Mixed mode

In a situation where more than one mode acts simultaneously, the damage starts propagating even before one of the limit tractions for pure mode load-

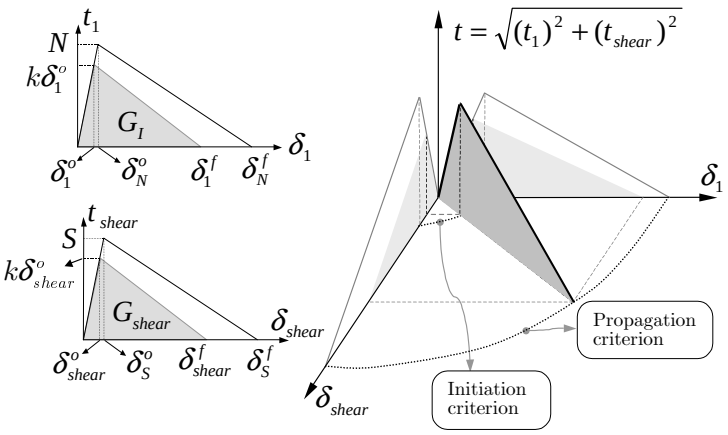

Fig. 2. Mixed-mode behaviour for the bi-linear law

ing (N or S) is attained individually—Fig. 2. In order to analyze this situation, the shear relative-displacement, δ_{shear}, and the magnitude of the relative displacement, δ, are defined as

$$\delta_{shear} = \sqrt{(\delta_2)^2 + (\delta_3)^2}, \qquad \delta = \sqrt{\langle \delta_1 \rangle^2 + (\delta_{shear})^2} \tag{3}$$

where the operator $\langle \cdot \rangle$ is the Mc-Cauley bracket defined as $\langle x \rangle = \max\{0, x\}$, $x \in \mathbb{R}$. The shear traction is defined as

$$t_{shear} = \sqrt{(t_2)^2 + (t_3)^2} \tag{4}$$

and the participation of the different modes β, is defined as

$$\beta = \max\left\{0, \frac{\delta_{shear}}{\delta_1}\right\}. \tag{5}$$

The onset relative-displacement, δ^o, is defined by a mixed-mode *initiation* criterion and the final relative-displacement, δ^f, is defined by a mixed-mode *propagation* criterion.

2.2.1 Mixed-mode initiation criterion

The following quadratic delamination criterion is used, for it has proven to be suitable for delamination onset prediction in composite materials by other authors [14–16]:

$$\left(\frac{\langle t_1 \rangle}{N}\right)^2 + \left(\frac{t_{shear}}{S}\right)^2 = 1. \tag{6}$$

As tractions are a function of the relative displacements, the previous criterion may be expressed in terms of relative displacements resulting in

$$\delta^o = \begin{cases} \delta_S^o \delta_N^o \sqrt{\dfrac{1+\beta^2}{\left(\delta_S^o\right)^2 + \left(\beta \delta_N^o\right)^2}} \Leftarrow \delta_1 > 0 \\ \\ \delta_S^o \Leftarrow \delta_1 \leq 0. \end{cases} \tag{7}$$

2.2.2 Mixed-mode propagation criterion

The mixed-mode propagation criterion establishes the state of complete decohesion for different ratios of applied mode I and shear mode energy release rates. There are several criteria that establish mixed-mode propagation. One of these, the power law criterion [7], can be expressed as

$$\left(\frac{G_I}{G_{Ic}}\right)^\alpha + \left(\frac{G_{shear}}{G_{Sc}}\right)^\alpha = 1. \tag{8}$$

Consider the energy absorbed up to the complete decohesion in a mixed-mode loading situation, for each mode. As the tractions are a function of the relative displacements, these energies may be expressed in terms of relative displacements. The energy absorbed by each mode in a mixed-mode loading is (Fig. 2)

$$G_I = \frac{k \delta_1^o \delta_1^f}{2} \quad \text{and } G_{shear} = \frac{k \delta_{shear}^o \delta_{shear}^f}{2}. \tag{9}$$

Introducing Eq. 9 in the expression of the power law criterion, Eq. 8, the expression for δ^f can be obtained as

$$\delta^f = \begin{cases} \dfrac{2\left(1+\beta^2\right)}{k\delta^o}\left[\left(\dfrac{1}{G_{Ic}}\right)^{\alpha}+\left(\dfrac{\beta^2}{G_{Sc}}\right)^{\alpha}\right]^{-1/\alpha} \Leftarrow \delta_1 > 0 \\ \\ \delta_S^{\,f} \Leftarrow \delta_1 \leq 0. \end{cases} \tag{10}$$

For most carbon/epoxy composites, the mixed-mode data can be accurately represented using $1 \leq \alpha \leq 2$.

The B-K criterion (Benzeggagh and Kenane, [17]) uses the parameter η to describe the mixed-mode interface behaviour:

$$G_{Ic} + \left(G_{Sc} - G_{Ic}\right)\left(\frac{G_{shear}}{G_I + G_{shear}}\right)^{\eta} = G_I + G_{shear}. \tag{11}$$

Proceeding as before, but now using this criterion, the expression for the final relative displacement is obtained as

$$\delta^f = \begin{cases} \dfrac{2}{k\delta^o}\left[G_{Ic} + \left(G_{Sc} - G_{Ic}\right)\left(\frac{\beta^2}{1+\beta^2}\right)^{\eta}\right] \Leftarrow \delta_1 > 0 \\ \\ \delta_S^{\,f} \Leftarrow \delta_1 \leq 0. \end{cases} \tag{12}$$

2.3 Constitutive law

In order to account for irreversibility, the maximum over time value of the mixed-mode displacement is defined as, at time τ,

$$\delta^{\max}(\tau) = \max_{\tau' \leq \tau}\left\{\delta\left(\tau'\right)\right\}. \tag{13}$$

Neglecting the interpenetration that occurs in the eventuality of compression,

the constitutive law could be expressed very simply as

$$t_i = (1-d)\, k\delta_i \qquad \text{(no sum in } i\text{)} \tag{14}$$

where only one damage variable is used, and is defined as

$$d = \begin{cases} 0 \Leftarrow \delta^{\max} \leq \delta^o \\ \frac{\delta^f(\delta^{\max}-\delta^o)}{\delta^{\max}\left(\delta^f-\delta^o\right)} \Leftarrow \delta^o < \delta^{\max} \leq \delta^f \\ 1 \Leftarrow \delta^{\max} \geq \delta^f . \end{cases} \tag{15}$$

The expression for the damage variable above results directly from the definition of the onset and final relative-displacements, and the bilinear shape for the constitutive law. From Eq. 15, it follows that $d \in [0,1]$.

In order to avoid interpenetration for compression situations, a simple contact logic already available in most FE codes could be used. Instead, the following condition is be added to Eq. 14:

$$t_1 = k\delta_1 \Leftarrow \delta_1 \leq 0. \tag{16}$$

This constitutive law in Eq. 16 has only one damage variable d, and, in a mixed-mode situation, implies that the state of complete decohesion is attained *at the same time* for opening and shear loading.

2.4 Comparison to other formulations

The decohesion formulation presented is compared to the one proposed by Crisfield and co-workers in Refs. [7,8,13]. In those references, the following

relation between relative displacements and tractions is proposed:

$$t_1 = \left(1 - \frac{\kappa}{1+\kappa}\frac{\delta_N^f}{\delta_N^f - \delta_N^o}\right) k\delta_1 \tag{17}$$

$$t_{shear} = \left(1 - \frac{\kappa}{1+\kappa}\frac{\delta_S^f}{\delta_S^f - \delta_S^o}\right) k\delta_{shear} \tag{18}$$

with

$$\kappa = \left\langle \left[\left(\frac{\langle \delta_1 \rangle}{\delta_N^o} \right)^{2\alpha} + \left(\frac{\delta_{shear}}{\delta_S^o} \right)^{2\alpha} \right]^{1/(2\alpha)} - 1 \right\rangle . \tag{19}$$

This formulation verifies the power law for damage propagation, as expressed in Eq. 8. Fig. 3 compares the applications of both implementations in a mixed-mode loading situation with $\beta = 1/2$, for an interface with the following properties: $G_{Ic} = 0.7\,\mathrm{kJ/m^2}$, $G_{IIc} = 1.7\,\mathrm{kJ/m^2}$, $N = 80\,\mathrm{kJ/m^2}$, $S = 100\,\mathrm{kJ/m^2}$ and $k = 1 \times 10^5\,\mathrm{N/mm^3}$. For this comparison, the value $\alpha = 1$ is used for both formulations, as, for this case, the damage onset criterion expressed in Eq. 6 is also satisfied. Note that when damage starts propagating, the complete definition of the model requires the determination of the two different variables δ_1^f and δ_{shear}^f. However, only one equation is available: the one that results from the application of a propagation criterion. The other condition, implicitly considered in the model presented, is that the interface should attain the state of complete decohesion at the same time for normal and shear components of the traction, as can be observed in Fig. 3. On the other hand, for the model proposed in Refs. [7,8,13], complete decohesion is attained at different times for the opening and shear modes. In Ref. [13], it is recognized that this goes against experimental evidence; it is however argued that this problem can be simply overcome by considering different penalty stiffness values for mode I and mode II, so as to achieve $\delta_N^o/\delta_N^f = \delta_S^o/\delta_S^f$. All formulations presented in the present paper avoid this requirement.

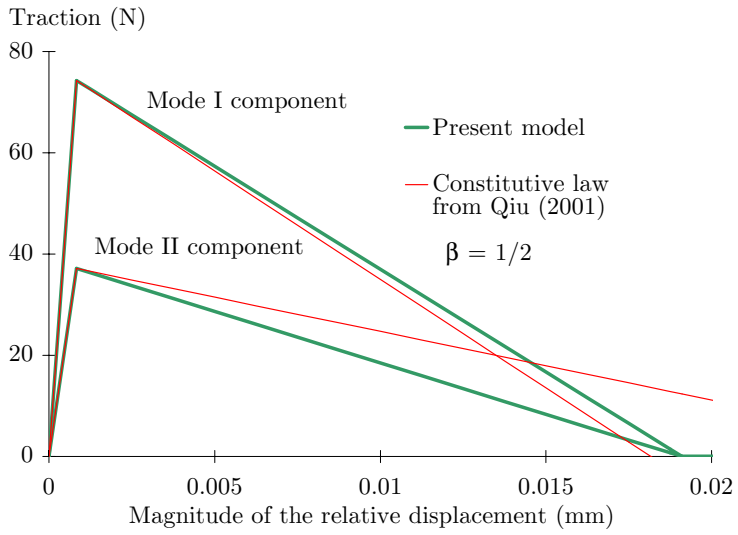

Fig. 3. Comparison of two different decohesion models in mixed mode

2.5 Varying mode ratio

In this formulation, the irreversibility of damage is considered through the definition of the maximum magnitude of the relative displacement (Eq. 13).

Consider a situation where the mode ratio at a given material point is constant in time. In this case, if unloading occurs after damage onset, then the point will linearly unload towards the origin and the maximum relative displacement that once existed at that point is recorded in the variable $\delta^{\max}$. When re-loading, no energy is absorbed until $\delta^{\max}$ is reached again. When complete decohesion occurs, the energy absorbed is the one defined by the propagation criterion, and does not depend on the loading/unloading sequence.

Consider now a more generic situation, where the mode ratio (at a given point) does change throughout the loading, in the damage propagation phase, Fig. 4. In this figure, a point has been loaded in mode I (vertical axis) and damage started propagating until it reached the point denoted by '1'. Suppose that

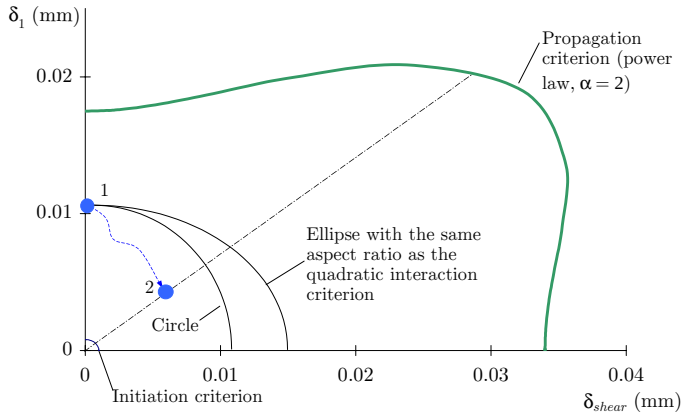

Fig. 4. Varying mode ratio at a point

in a numeric incremental implementation, the next equilibrium point is '2'. There is no trivial answer to what the memory of damage would be for this new mode ratio, and how much energy should still be available to be absorbed.

One possibility to address this issue in a decohesion formulation is that, at any load step, the maximum mixed-mode displacement is considered to provide a memory of the damage evolution, regardless of the mode ratio. In Fig. 4, this methodology is represented by the circle drawn from the initial point '1'. Another possibility, from Refs. [8,13], consists in storing the maximum value in time of the variable κ in Eq. 19. This approach is represented in Fig. 4 for the particular case of $\alpha = 1$, by the ellipse starting from point '1'. Note that, as long as the mode ratio does not change too much, then the two approaches are very similar.

2.6 Implementation

The decohesion model presented has been implemented in LS-Dyna [12] as a user material within a brick element. This approach for the implementation

has the implication of requiring to model the resin rich layer (for the case of delaminations) as a non-zero thickness medium. However, the resin rich layer has, in fact, a finite thickness and mass scaling can be used to obtain faster solutions when applying the decohesion element to quasi-static situations. Note that the volume associated with the decohesion element can in fact be set to be very small by using a small thickness (0.01 to 0.001mm) and the element's kinetic energy arising from this be still several orders of magnitude below its internal energy, which is an important consideration for quasi-static analyses.

3 Two other constitutive laws

3.1 Introduction

The bilinear constitutive law presented in the previous section allows the modelling of delamination in composite materials and has been successfully used by several authors in implicit analyses [1,6,9]. However, it will become evident in the next section of this paper that the two discontinuities existing in the bilinear law (at peak value and complete decohesion) generate numerical instabilities in an explicit implementation. In certain situations, a stress wave is generated at those points, and this excites high-frequency vibrations that completely break the decohesion elements in the vicinity. It is possible to overcome this problem by using damping algorithms, higher mesh refinement, lower interface strength, higher fracture toughness or lower load-rate. However, the particular finite element model that is not affected by these shock waves is not always straightforward to define.

For those reasons, two alternative constitutive laws are proposed and imple-

mented in LS-Dyna [12]. The shape of the first law is a curve, and is defined by a third order polynomial function as proposed in Refs. [18]:

$$t = \frac{27}{4} t^o \left(1 - \frac{\delta}{\delta^f}\right)^2 \frac{\delta}{\delta^f}. \tag{20}$$

It can be easily shown that the maximum value of the traction in Eq. 20 is t^o, which corresponds to damage onset. It can also be shown that the maximum traction corresponds to a relative displacement $\delta = \delta^f/3$. The final displacement in a single-mode loading can be related to t^o and the energy dissipated per unit area G_c by

$$\delta^f = \frac{48}{27} \frac{G_c}{t^o}. \tag{21}$$

The function in Eq. 20 has no discontinuities, and the slope at complete decohesion is zero, which renders the complete failure of the element much smoother—Fig. 5(a) and (b). In order to introduce a damage variable (which is useful to define the mixed-mode behaviour, irreversibility, for post-processing, and for uniformity of the implementation), Eq. 20 can be expressed as

$$t = k\,(1 - d)\,\delta \tag{22}$$

where $k = 27 t_o / 4\delta^f$, $d = 1$ for $\delta > \delta^f$, and

$$d = 2\frac{\delta}{\delta^f} - \left(\frac{\delta}{\delta^f}\right)^2 \quad \text{for} \quad \delta \leq \delta^f. \tag{23}$$

The second alternative constitutive law proposed and implemented in LS-Dyna [12] is similar to the bilinear, in the sense that it is characterized by a linear-elastic behaviour before failure onset. However, it is also similar to the third order polynomial constitutive law, in the sense that discontinuities are smoothed by using a third-order damage variable. The constitutive law,

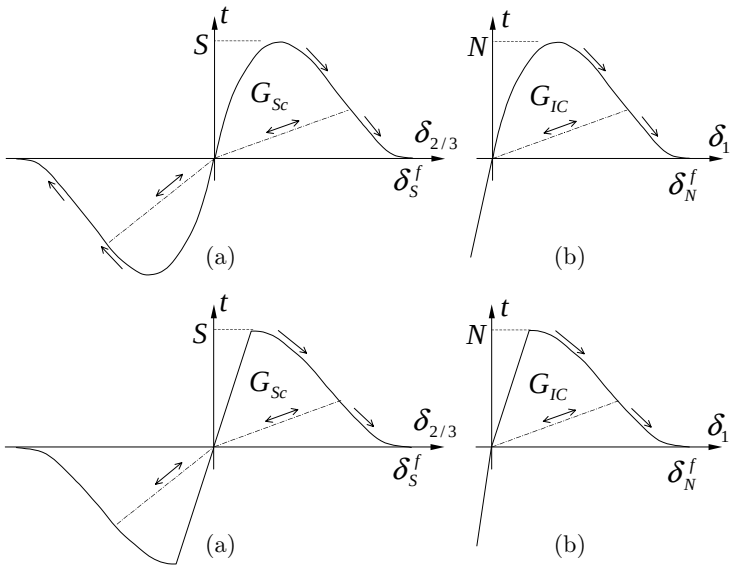

Fig. 5. Third-order polynomial constitutive law (a) shear mode and (b) opening mode; linear/ polynomial constitutive law c) shear mode and (d) opening mode

shown in Fig. 5(c) and (d), can be expressed by Eq. 22, but with the damage variable defined as $d = 0$ for $\delta \leq \delta^o$, $d = 1$ for $\delta > \delta^f$, and

$$d = 1 - \frac{\delta^o}{\delta}\left[1 + \left(\frac{\delta - \delta^o}{\delta^f - \delta^o}\right)^2 \left(2\frac{\delta - \delta^o}{\delta^f - \delta^o} - 3\right)\right] \quad \text{for} \quad \delta^o < \delta \leq \delta^f. \qquad (24)$$

The constitutive law defined by Eqs. 22 and 24 has zero slope at failure onset, conducing to a discontinuity which is less severe than the one existing for the bilinear formulation, and the slope at complete decohesion is zero, which renders complete failure smoother.

3.2 Constitutive law

The bilinear formulation presented in the previous section is based on previous work [1,9,6], and for consistency with that work, the mixed-mode ratio was defined as $\beta = \delta_{shear}/\delta_1$. However, this definition implies that a division by zero occurs for pure shear mode loading, which has to be considered as a particular

case in the numerical implementation. An alternative definition is therefore used in this section, which avoids this division by zero: $\theta = \text{acos}\,\langle\delta_1\rangle\,/\delta$, $\theta \in [0, \pi/2]$. The contribution of the different shear components is defined as $\omega = \text{atan}\,\delta_3/\delta_2$, $\omega \in [0, 2\pi[$.

The constitutive law of the interface element, expressed on the direction of the relative displacement, is defined as

$$t = k_{pos}\,(1 - d)\,\delta \tag{25}$$

where k_{pos} is an input parameter for the bilinear and the linear/polynomial constitutive laws, but is computed as $k_{pos} = 27t_o/4\delta^f$ for the third order polynomial law. The traction components are recovered as

$$t_1 = t\cos\theta, \qquad t_{shear} = t\sin\theta \tag{26}$$

$$t_2 = t_{shear}\cos\omega, \qquad t_3 = t_{shear}\sin\omega \tag{27}$$

with this condition added to prevent interpenetration:

$$t_1 = k_{neg}\delta_1 \Leftarrow \delta_1 \leq 0 \tag{28}$$

where k_{neg} is the penalty stiffness, also given to the model as an input parameter.

3.3 Mixed-mode behaviour

3.3.1 Initiation criterion

The initiation criterion used in the bilinear constitutive law of the previous section, Eq. 6, is also used here. When applied to this formulation, the expres-

sion for the magnitude of the onset traction is

$$t^o = \left[\left(\frac{\cos\theta}{N} \right)^2 + \left(\frac{\sin\theta}{S} \right)^2 \right]^{-1/2}. \tag{29}$$

For the bilinear and the linear/polynomial constitutive laws, the onset relative displacement needs to be defined and is obtained as

$$\delta^o = t^o / k_{pos} \tag{30}$$

where k_{pos} is the elastic stiffness.

3.3.2 Propagation criterion

Using the power law (Eq. 8) for propagation criterion, and using the definition of the participation of each mode ratio θ, Eq. 8 can be manipulated to obtain the fracture toughness G_c as

$$G_c = \left[\left(\frac{\cos^2\theta}{G_{Ic}} \right)^{\alpha} + \left(\frac{\sin^2\theta}{G_{Sc}} \right)^{\alpha} \right]^{-1/\alpha}. \tag{31}$$

The B-K criterion (Eq. 11) an also be used instead of the power law, resulting in

$$G_c = G_{Ic} + (G_{Sc} - G_{Ic}) \left(\sin^2\theta \right)^{\eta}. \tag{32}$$

The final relative-displacement can then be obtained as

$$\delta^f = \begin{cases} \dfrac{2G_c}{t^o} \quad \text{(Bilinear and linear/ polyn. laws)} \\ \\ \dfrac{48}{27}\dfrac{G_c}{t^o} \ (3^{rd} \text{ order polynomial law}). \end{cases} \tag{33}$$

3.4 Irreversibility

Irreversibility can be addressed by storing the maximum value in time of the magnitude of the relative displacement δ. This approach was followed in the previous section, for consistency with the work on which it was based [1,9,6]. Other similar approaches are possible, such as storing the maximum value in time of the variable δ/δ^o or of the variable δ/δ^f. With any of these approaches however, it cannot be always and simultaneously guaranteed that a point at the stage of damage propagation will not become completely undamaged or fully damaged, just as a result of a change in the mode ratio. Also, with some of the previous approaches, and in particular with the one implemented in the previous section, a fully damaged point could become only partially damaged as a result of just a change in the mode ratio. These assertions can be better visualized using Fig. 4.

An approach that avoids the mentioned limitation, and which is eventually more intuitive, consists of storing the maximum value in time of the damage variable itself. With the latter approach, the instantaneous value of the damage variables are defined as

$$d_{inst} = \begin{cases} 0 \Leftarrow \delta \leq \delta^o \\ \frac{\delta^f(\delta-\delta^o)}{\delta\left(\delta^f-\delta^o\right)} \Leftarrow \delta^o < \delta \leq \delta^f \quad \text{(Bilinear law)} \\ 1 \Leftarrow \delta \geq \delta^f \end{cases} \tag{34}$$

$$d_{inst} = \begin{cases} 2\frac{\delta}{\delta^f} - \left(\frac{\delta}{\delta^f}\right)^2 \Leftarrow \delta \leq \delta^f \\ 1 \Leftarrow \delta \geq \delta^f \end{cases} \quad (3^{rd} \text{ order polynomial law}) \tag{35}$$

$$d_{inst} = \begin{cases} 0 \Leftarrow \delta \leq \delta^o \\ 1 - \frac{\delta^o}{\delta}\left[1 + \left(\frac{\delta-\delta^o}{\delta^f-\delta^o}\right)^2\left(2\frac{\delta-\delta^o}{\delta^f-\delta^o} - 3\right)^2\right] \Leftarrow \delta^o < \delta \leq \delta^f \quad \text{(Linear/polyn. law)} \\ 1 \Leftarrow \delta \geq \delta^f \end{cases} \tag{36}$$

and the damage variable itself is obtained from the instantaneous value as

$$d(\tau) = \max_{\tau' < \tau} \{d(\tau')\}\,. \tag{37}$$

For the 3^{rd} order polynomial constitutive law, Eq. 37 can be modified so that a reversible non-linear elastic behaviour exists before damage onset, resulting in

$$d(\tau) = \begin{cases} d_{inst}(\tau) \Leftarrow d \leq 5/9 \\ \max_{\tau' < \tau} \{d_{inst}(\tau')\} \Leftarrow d > 5/9 \end{cases} \quad (3^{rd} \text{ order polynomial}). \tag{38}$$

3.5 Implementation

The third-order polynomial decohesion model presented has also been implemented in LS-Dyna [12] as a user material within a brick element.

4 Comparison

The three different decohesion-element constitutive laws implemented in LS-Dyna are compared in test cases which are designed to test the limits of their stability. For decohesion elements implemented in explicit codes, stability is affected negatively by coarse meshes, high maximum tractions in the interface

and low fracture toughness (because these factors result in fewer elements in the cohesive zone). Discontinuity points in the constitutive law, like those in the bilinear formulation, also affect stability negatively, as shock waves are generated when the elements fail; this effect is found to be more pronounced at higher load-rates, probably due to the higher kinetic energy of the model [19].

One example examining the limits of stability of the three decohesion laws consists of a pure mode I DCB test of a carbon-PEEK composite, with material properties $E = 150\,\mathrm{GPa}$ and $G_{Ic} = 0.7\,\mathrm{kJ/m^2}$. For the maximum traction, two values $N = 50\,\mathrm{MPa}$ and $N = 80\,\mathrm{MPa}$ are compared. The penalty stiffness used is $k = k_{pos} = k_{neg} = 1 \times 10^5\,\mathrm{N/mm^3}$. The specimen is $25\,\mathrm{mm}$ wide and $3\,\mathrm{mm}$ thick, with a pre-crack length of $33\,\mathrm{mm}$. The length of each decohesion element is $0.37\,\mathrm{mm}$ and only one integration point per element is used. A high displacement-rate of $4000\,\mathrm{mm/s}$ is applied to the specimen.

Fig. 6(a) presents the load-displacement curve obtained with the three constitutive laws implemented, for a maximum traction $N = 50\,\mathrm{MPa}$, and Fig. 6(b) presents the same results for a maximum traction $N = 80\,\mathrm{MPa}$. Both figures show the analytical curve corresponding damage propagation, assuming simple beam theory and treating the specimen arm as built-in at the crack tip.

While all formulations were found to be stable at lower imposed displacement-rates, the bilinear formulation results in a severe instability once the crack starts propagating, for this fast loading. However, the other constitutive laws are able to model the smooth, progressive crack propagation. The vibrations observed during crack propagation for the linear and for the linear/ polynomial

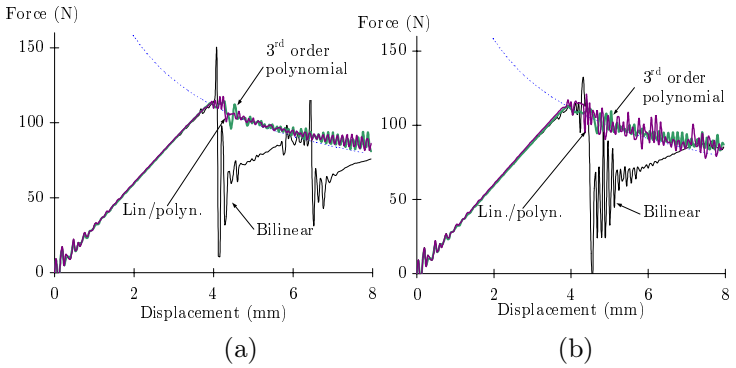

Fig. 6. Comparison of the load displacement curves obtained with different interface models, for (a) $N = 50\,\mathrm{MPa}$ and (b) $N = 80\,\mathrm{MPa}$

laws are more pronounced for higher maximum tractions in the interface. For the bilinear law, higher tractions resulted in a more severe instability (bigger crack jump).

5 Applications

Mode I (DCB, [20]), mode II (4ENF, [21]) and mixed mode (MMB, [22]) tests were carried [23] on specimens manufactured from carbon-epoxy prepreg (T300/913), supplied by Hexcel. The main results from these tests are presented graphically in Fig. 7. To characterize the mixed-mode behaviour, the power law with coefficient $\alpha = 1.21$ was found to give the best fit to the mixed-mode data. This value of α has therefore been used in the simulations. The average mode I and mode II fracture toughness were determined as $G_{Ic} = 0.258\,\mathrm{kJ/m^2}$ and $G_{IIc} = 1.08\,\mathrm{kJ/m^2}$.

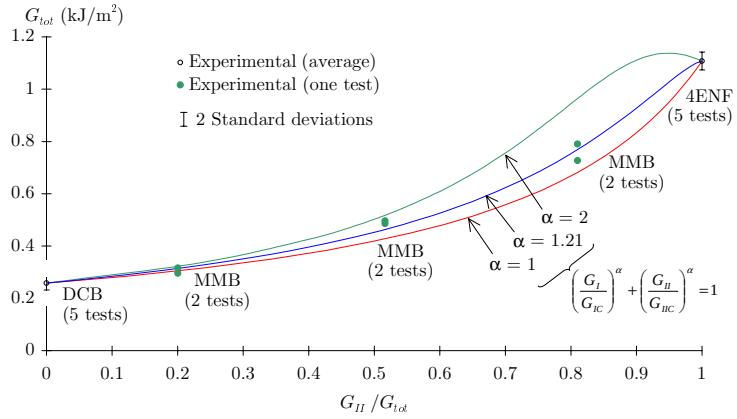

Fig. 7. Total fracture toughness, as a function of mode ratio

5.1 Mode I

One of the DCB specimens from the mentioned test program [23] was chosen to be simulated. The specimen was 20 mm wide, 3.1 mm thick and the pre-crack length was 53 mm —Fig. 8. The average mode I fracture toughness registered during the test is $G_{Ic} = 0.268\,\mathrm{kJ/m^2}$ and the flexural Young's modulus is $E = 119\,\mathrm{GPa}$. The maximum mode I traction was arbitrarily taken as $N = 60\,\mathrm{MPa}$. The minimum decohesion-element length in the numerical model was 0.2 mm. A displacement-rate of 560 mm/s was applied to the appropriate points of the model. The load vs. displacement curves obtained from the simulation are presented in Fig. 9, together with experimental data and the analytical solution for propagation.

It can be observed that the numerical curves slightly over-estimate the load for large displacements. The error in the fracture energy absorbed by each failed element is monitored and found to be under 0.0025% for all formulations. The difference between analytical and numerical is thus essentially due to other factors which include kinetic, hourglass-control and damping energy in the model, as well as accumulation of round-off errors during the analysis.

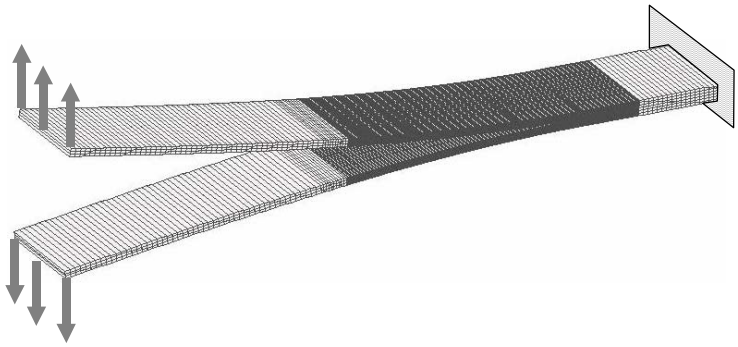

Fig. 8. Numerical model of a DCB specimen

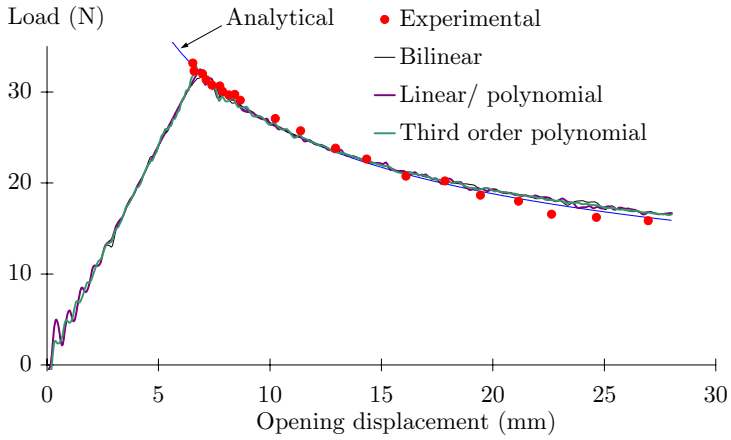

Fig. 9. Experimental, analytical and numerical load-displacement curves for a DCB specimen

5.2 Mode II

A particular 4ENF specimen from the mentioned test program [23] was chosen to be simulated. The specimen was 20 mm wide, 3.1 mm thick and the pre-crack length was 25 mm. Part of the loading rig was modelled as well, in order to account correctly for the boundary conditions, as shown in Fig. 10. The measured fracture toughness, $G_{IIc} = 1.11\,\mathrm{kJ/m^2}$, was used in the simulation, and the flexural modulus was taken as $E = 137\,\mathrm{GPa}$. The maximum mode II traction was arbitrarily taken as $S = 60\,\mathrm{MPa}$. The minimum decohesion element length was 0.5 mm. A displacement-rate of 240 mm/s was applied to

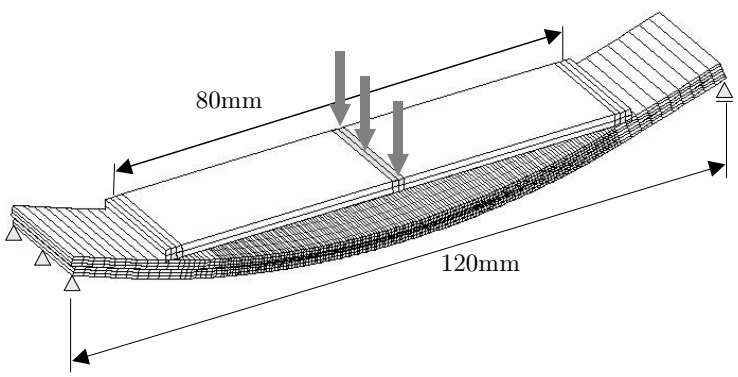

Fig. 10. Mesh and loading body for the 4ENF specimen

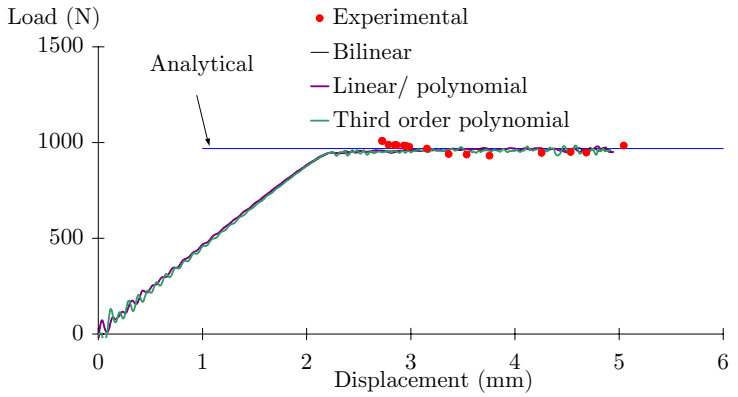

Fig. 11. Experimental, analytical and numerical load-displacement curves, for an ENF specimen

the appropriate points of the model.

The maximum error in the energy absorbed by each element is under 1% for all formulations. With the exception of the harmonic vibrations related to the dynamic loading, the numerical results fit very well the analytical and experimental ones, Fig. 11.

5.3 Mixed mode

The simulation of an MMB test also requires modelling of the test fixture, as shown in Fig. 12. The specimen modelled was 20 mm wide, 3.1 mm thick

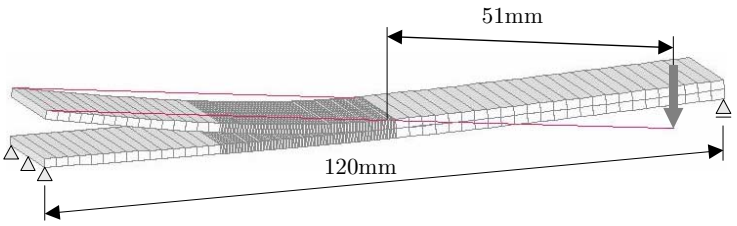

Fig. 12. Finite element model of the MMB test and boundary conditions

and the pre-crack length was 33 mm . The distances between loading points are shown in Fig. 12. The fracture toughness values used in this simulation were an average of the tests performed [23]: $G_{Ic} = 0.258\,\mathrm{kJ/m^2}$, $G_{IIc} = 1.108\,\mathrm{kJ/m^2}$, and, as reported earlier, the power law parameter α was determined to be 1.21. The flexural modulus obtained from the test was $E = 112\,\mathrm{GPa}$. The maximum mode I and mode II tractions were arbitrarily taken as $N = S = 60\,\mathrm{MPa}$. The minimum decohesion element length was 0.25 mm . A displacement-rate of 60 mm/s was applied to the appropriate points of the model.

There is a good agreement between the numerical, analytical and experimental data, as shown in Fig. 13. Note that in this case, a significant part of the difference between numerical and analytical results from two factors not present in pure-mode loading situations: the decohesion element (i) interpolates the mixed-mode fracture toughness using the power law, and (ii) obtains the mode ratio from the ratio of relative displacements, and the latter ratio might be influenced by the vibrations in the model.

6 Conclusions

Three different constitutive laws were implemented within an interface element formulation into the industrial standard LS-Dyna [12] explicit dynamic code. The formalism used is relatively simple and modular, allowing other

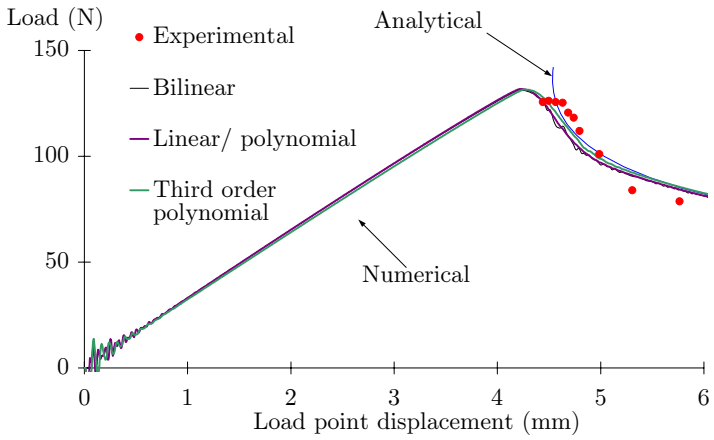

Fig. 13. Experimental, analytical and numerical load-displacement curves for an MMB specimen

constitutive laws to be added easily. Initiation criteria, which define the maximum traction in mixed-mode situations, as well as propagation criteria, which define the energy absorbed in mixed-mode situations, can also be added taking advantage of the modularity of the implementation.

When under less favorable numerical conditions (e.g. DCB loaded at 4000mm/s), it was observed that the discontinuities existing in the bilinear constitutive law resulted in instabilities. These were not observed for the 3^{rd} order polynomial or linear-polynomial laws. However, all formulations were shown to model appropriately mode I, mode II and mixed mode I and II quasi-static crack propagation problems at lower loading rates.

The decohesion element, implemented in LS-Dyna, were shown to acurately model a range of static delamination problems, using a dynamic relaxation technique. The decohesion element can now be applied to a range of impact and crash problems, which may in addition involve in-plane damage. Other applications include modelling compression after impact (CAI) and the propagation of any delaminations from the initial impact.

References

[1] M. F. S. F. de Moura, J. P. Gonçalves, A. T. Marques, P. T. de Castro, Prediction of compressive strength of carbon-epoxy laminates containing delaminations by using a mixed-mode damage model, Composite Structures 50 (2000) 151–157.

[2] P. P. Camanho, C. G. Dávila, Mixed-mode decohesion finite elements for the simulation of delamination in composite materials, Tech. Rep. NASA/TM-2002-211737, National Aeronautics and Space Administration, U. S. A. (2002).

[3] Y. Mi, M. A. Crisfield, Analytical derivation of load/ displacement relationship for the DCB and MMB and proof of the FEA formulation, Tech. rep., Internal Report, Department of Aeronautics, Imperial College London (April 1996).

[4] O. Allix, A. Corigliano, Geometrical and interfacial non-linearities in the analysis of delamination in composites, International Journal of Solids and Structures 36 (1999) 2189–2216.

[5] M. Ortiz, A. Pandolfi, Finite-deformation irreversible cohesive elements for three-dimensional crack-propagation analysis, International Journal for Numerical Methods in Engineering 44 (1999) 1267–1282.

[6] P. P. Camanho, C. G. Dávila, M. F. de Moura, Numerical simulation of mixed-mode progressive delamination in composite materials, Journal of Composite Materials 37 (16) (2003) 1415–1438.

[7] Y. Mi, M. A. Crisfield, A. O. Davies, Progressive delamination using interface elements, Journal of Composite Materials 32 (14) (1998) 1246–1272.

[8] Y. Qiu, M. A. Crisfield, G. Alfano, An interface element formulation for the simulation of delamination with buckling, Engineering Fracture Mechanics 68 (2001) 1755–1776.

[9] S. T. Pinho, Crush simulation and energy absorption of composite tubes, Master's thesis, University of Porto, Faculty of Engineering, Portugal (September 2002).

[10] A. F. Johnson, A. K. Pickett, P. Rozycki, Computational methods for predicting impact damage in composite structures, Composites Science and Technology 61 (2001) 2183–2192.

[11] A. K. Pickett, Review of finite element simulation methods applied to manufacturing and failure prediction in composite structures, Applied Composite Materials 9 (2002) 43–58.

[12] Livermore Software Technology Corporation, California, USA, LS-Dyna 970 (2003).

[13] G. Alfano, M. A. Crisfield, Finite element interface models for the delamination analysis of laminated composites: mechanical and computational issues, International Journal for Numerial Methods in Engineering 50 (2001) 1701–1736.

[14] M. F. S. F. de Moura, J. P. Gonçalves, A. T. Marques, P. T. de Castro, Elemento finito isoparamétrico de interface para problemas tridimensionais, Revista Internacional de Métodos Numéricos Para Cálculo e Diseño en Ingeniería 14 (1996) 447–466.

[15] P. P. Camanho, M. F. de Moura, Simulation of interlaminar damage using decohesion elements, in: 13th International Conference on Composite Materials, Beijing, China, 2001.

[16] C. G. Dávila, P. P. Camanho, M. F. de Moura, Mixed-mode decohesion elements for analyses of progressive delamination, in: 42nd AIAA/ ASME/ ASCE/ AHS/ ASC Structures, Structural Synamics, and Materials Conference and Exhibit, Seattle, 2001.

[17] M. L. Benzeggagh, M. Kenane, Measurement of mixed-mode delamination fracture toughness of unidirectional glass/epoxy composites with mixed-mode bending apparatus, Composites Science and Technology 56 (4) (1996) 439–449.

[18] V. Tvergaard, Effect of fibre debonding in a whisker-reinforced metal, Materials Science and Engineering A 125 (1990) 203–213.

[19] S. T. Pinho, L. Iannucci, P. Robinson, Modelling delamination in an explicit FE code using 3D decohesion elements, in: Composites Testing and Model Identification, CompTest2004, Bristol, U.K., 21st-23rd September 2004.

[20] ASTM standard D 5528-94a, Standard test method for mode I interlaminar fracture touthness of unidirectional fiber-reinforced polymer matrix composites (1994).

[21] R. H. Martin, T. Elms, S. Bowron, Characterisation of mode II delamination using the 4ENF, in: I. of Materials London (Ed.), 4th European Conference on Composites: Testing and Standardisation, Lisbon, Portugal, 1998.

[22] ASTM Standard D6671-01, Standard test method for mixed mode i-mode II interlaminar fracture toughness of unidirectional fiber reinforced polymer matrix composites (2001).

[23] S. T. Pinho, MPhil to PhD transfer report: Formulation and implementation of a 3D decohesion element for delamination modelling in explicit FE codes (2003).